Ultrametricity in physics of complex systems: from proteins to quantum chaos.

Vladimir Al. Osipov

May 24, 2025

There are several motivations in physics and mathematics to investigate ultrametric and p-adic mathematical models.

- Breakdown of the Archimedean axiom at the Planck scale. The number field invariance principle: Fundamental physical laws should be invariant under the change of the number fields.
- Application of p-adic numbers to cryptography: they serve as a primitive in the selection of the secure elliptic curves allowing to solve the problem of counting the number of solutions in finite fields of the bivariate polynomial equations $P(X, Y) = 0$.
- Ultrametric spaces are adequate mathematical instrument for investigation of hierarchical structures appearing in some phenomena of the complex systems, where p-adics can be used as a toy model.

Complex System

The prototype of a completely disordered system (order 0) is the ideal gas; no information can be stored and its complexity is zero.
The prototype of a completely ordered system is the ideal crystal (order 1); no information can be stored and its complexity is zero.
A complex system is a system composed of many components that may interact with each other. The main question: How the system's parts give rise to the collective behaviours, and how the system interacts with the environment?

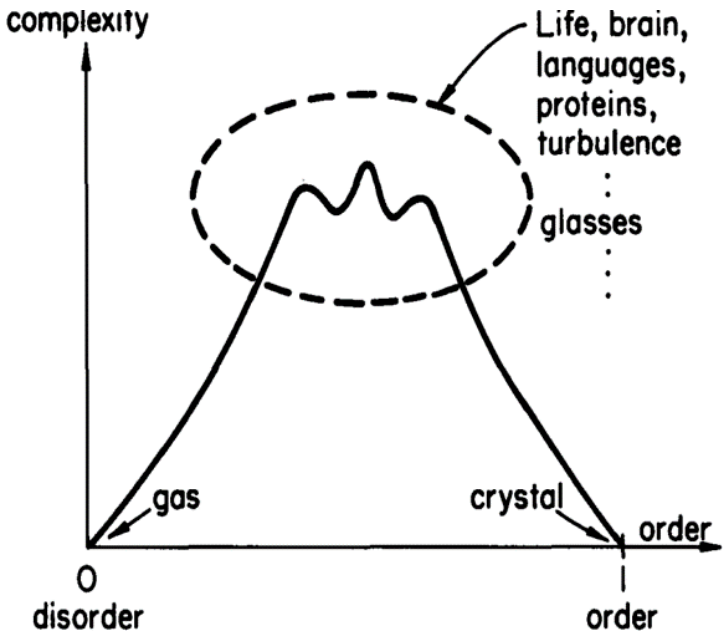

Spin glasses – a paradigmatic example of complex system

The spin-glass Hamiltonian

$$H\{\boldsymbol{\sigma}\} = -\sum_{i,j} J_{i,j}\sigma_i\sigma_j,$$

The coupling constants are randomly distributed values with respect to some given probability. The Sherrington-Kirkpatrick model (1975)

$$dP[J] = \prod_{i,j} \frac{dJ_{i,j}}{\sqrt{2\pi\Delta}} e^{-\frac{J_{i,j}^2}{2\Delta}}$$

Disordered interactions result in "frustration".

The signs along the edges indicate whether two neighboring spins prefer to point in the same (+) or opposite (-) directions. It is therefore impossible to satisfy all the couplings simultaneously on the square plaquette.

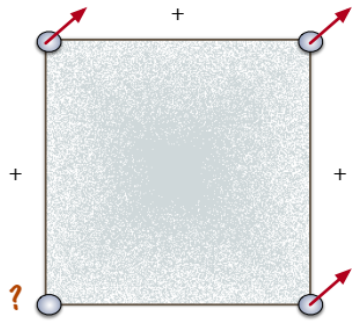

Hierarchical structure of the free-energy landscape

The history dependent thermodynamic effects lead to the picture of free-energy landscape of the hierarchically nesting metastable states (Dotsenko et al., 1990; Refregier et al., 1987).

At a fixed temperature T, the system evolution corresponds to the slow exploration of the numerous metastable states (at level T). When going from T to $T - \Delta T$, the free-energy valleys subdivide into smaller ones, separated by new barriers (level $T - \Delta T$).
For large enough ΔT (and in the limited experimental time window), the transitions can only take place between the sub valleys inside the main valleys, in such a way that the population rates of the main valleys are untouched, keeping the memory of the previous configuration at T.

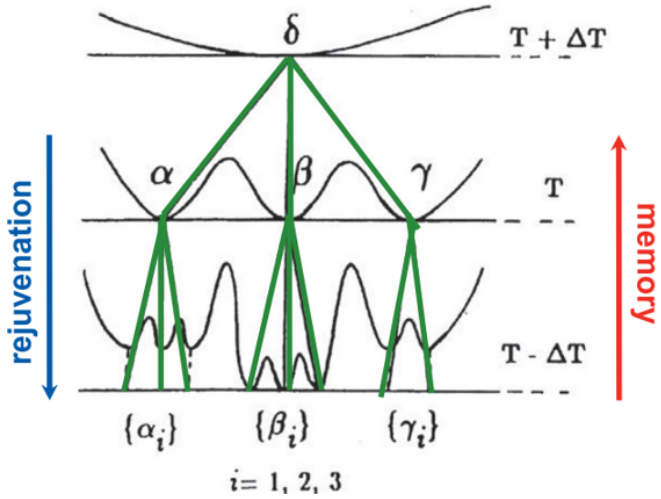

Replica trick

The averaged over disorder free energy

$$< F[J] >_J = -T < \log Z[J] >_J = -T \int dP[J] \log Z[J].$$

The replica method overcomes the difficulty of the calculation of the logarithm of the partition function Z by replacing it with n copies of Z through the identity

$$\log Z = \lim_{n \to 0} \frac{Z^n - 1}{n}$$

In the analysis n is taken to be integer, while the analytic continuation $n \to 0$ and the thermodynamic limit $N \to \infty$ are assumed.
Replicas have exactly the same coupling but evolves independently. The overlap parameter (i – the lattice index and α, β are replica indexes)

$$Q_{\alpha,\beta} = \frac{1}{N} \sum_{i=1}^{N} \sigma_i^\alpha \sigma_i^\beta, \quad 0 \leq Q_{\alpha,\beta} \leq 1.$$

One is searching for the saddle point solutions over Q.

Parisi Matrix

The completely broken replica symmetry solution is given by the Parisi matrix with block hierarchical structure, which possesses the *p*-adic parametrization.

$$Q_{\alpha,\beta} = \rho(|\ell(\alpha) - \ell(\beta)|_p), \quad \alpha, \beta \in \{1, 2, \ldots, p^\kappa\}$$

$$\ell: \quad \alpha = 1 + \sum_{i=1}^{\kappa} a_i p^{i-1} \longrightarrow \ell(\alpha) = p^{-\kappa} \sum_{i=1}^{\kappa} a_i p^{i-1},$$

$$0 \le a_i \le p-1, \quad \ell \in p^{-\kappa}\mathbb{Z}_p/\mathbb{Z}_p.$$

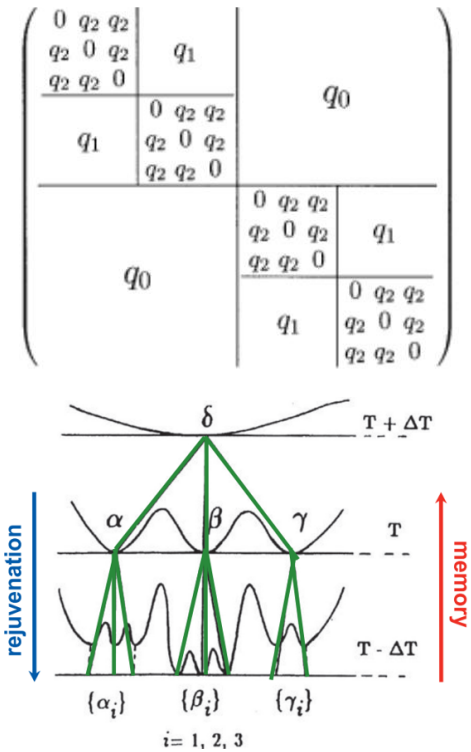

Dynamics on Ultrametric landscape

(Ogielski-Stein-Schreckenberg model 1985, revisited in 2003)

Given the hierarchical way in which the full-RSB construction is obtained the states (free energy minima) are organized in the similar hierarchical way.

- p-Adic model of ultrametric diffusion

$$\frac{\partial f(x,t)}{\partial t} = \int_{\mathbb{Q}_p} \rho(|x-y|_p)(f(y,t)-f(x,t))d\mu(y)$$

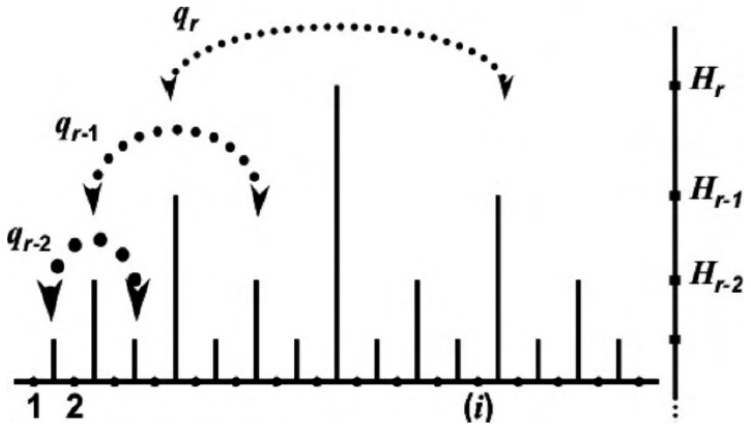

- Fourier transform

$$\frac{\partial \tilde{f}(\xi,t)}{\partial t} = \tilde{\rho}(|\xi|_p)\tilde{f}(\xi,t)$$

$$\tilde{\rho}(|\xi|_p) = \int_{\mathbb{Q}_p} \rho(|x|_p)(\chi_p(\xi x)-1)d\mu(x)$$

- Solution

$$f(x,t) = \int_{\mathbb{Q}_p} \tilde{g}(\xi)\exp\left\{\tilde{\rho}(|\xi|_p)t\right\}\chi_p(-\xi x)\,d\mu(\xi)$$

Dynamics on Ultrametric landscape

- The initial state decay problem: $R(t) = \int_{\mathbb{Z}_p} f(x,t)d\mu(x)$

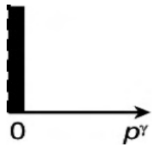

$$R(t) = (1-p^{-1})\sum_{\mu=0}^{+\infty} p^{-\mu}\exp(-\Lambda_\mu t) \qquad \Lambda_\mu = p^\mu\left[(1-p^{-1})\sum_{\gamma=1}^{+\infty} p^\gamma \rho(p^{\mu+\gamma}) + \rho(p^{\mu+1})\right]$$

- Landscape structure is encoded in the diffusion kernel. The simplest assumption is the standard Arrhenius law

$$\rho(|x-y|_p) = A(T)\frac{\exp\left(-\alpha\varphi(|x-y|_p)\right)}{|x-y|_p} \qquad \alpha = H_0/k_BT \qquad H_\gamma = H_0\varphi(p^\gamma)$$

A(T) is the typical rate, H_0 is the energy parameter. |x-y| in the denominator is the volume of the maximal basin of states separated by the corresponding activation barrier. The function phi determines the growth of the activation barriers (landscape structure).

Logarithmic landscape	$H_\gamma \sim \ln\gamma$		$\rho(\lvert x-y\rvert_p) = \frac{1}{\lvert x-y\rvert_p \ln^\alpha \lvert x-y\rvert_p}$
Linear landscape	$H_\gamma \sim \gamma$	V.Op.	$\rho(\lvert x-y\rvert_p) = \frac{1}{\lvert x-y\rvert_p^{\alpha+1}}$
Exponential landscape	$H_\gamma \sim e^\gamma$		$\rho(\lvert x-y\rvert_p) = \frac{\exp(-\alpha\lvert x-y\rvert_p)}{\lvert x-y\rvert_p}$

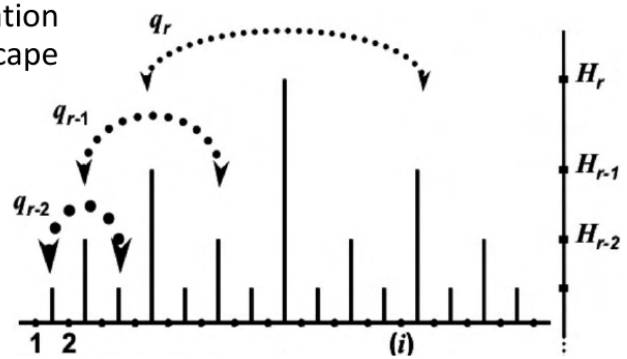

Dynamics on Ultrametric landscape

- The initial state decay problem: $R(t) = (1-p^{-1}) \sum_{\mu=0}^{+\infty} p^{-\mu} \exp(-\Lambda_\mu t)$

$$\Lambda_\mu = p^\mu \left[(1-p^{-1}) \sum_{\gamma=1}^{+\infty} p^\gamma \rho(p^{\mu+\gamma}) + \rho(p^{\mu+1}) \right]$$

Logarithmic landscape $H_\gamma \sim \ln \gamma$	$\rho(\lvert x-y\rvert_p) = \frac{1}{\lvert x-y\rvert_p \ln^\alpha \lvert x-y\rvert_p}$ **The relaxation follows the Kohlrausch law (stretched exponent)**	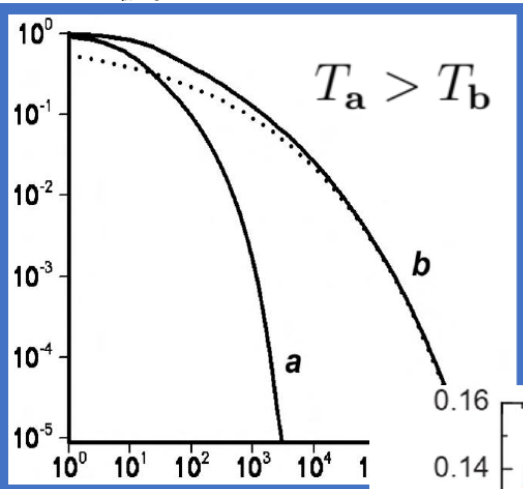
Linear landscape $H_\gamma \sim \gamma$	V.Op. $\rho(\lvert x-y\rvert_p) = \frac{1}{\lvert x-y\rvert_p^{\alpha+1}}$	
Exponential landscape $H_\gamma \sim e^\gamma$	$\rho(\lvert x-y\rvert_p) = \frac{\exp(-\alpha \lvert x-y\rvert_p)}{\lvert x-y\rvert_p}$	

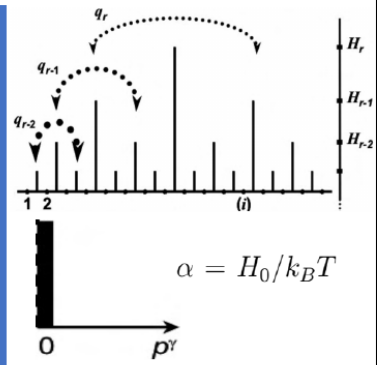

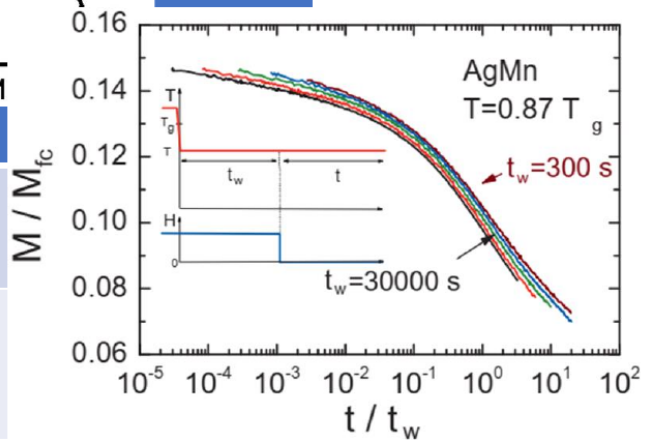

A Avetisov, A Kh Bikulov and V AI Osipov J. Phys. A: Math. Gen. 36 (2003) 4239–4246

Frauenfelder hypothesis

Frauenfelder hypothesis on hierarchical structure of the conformation substates (CS) in proteins.

- H. FRAUENFELDER,"*Function and Dynamics of Myoglobin*", *Annals of the New York Academy of Sciences, 504, 151-167*(1987).

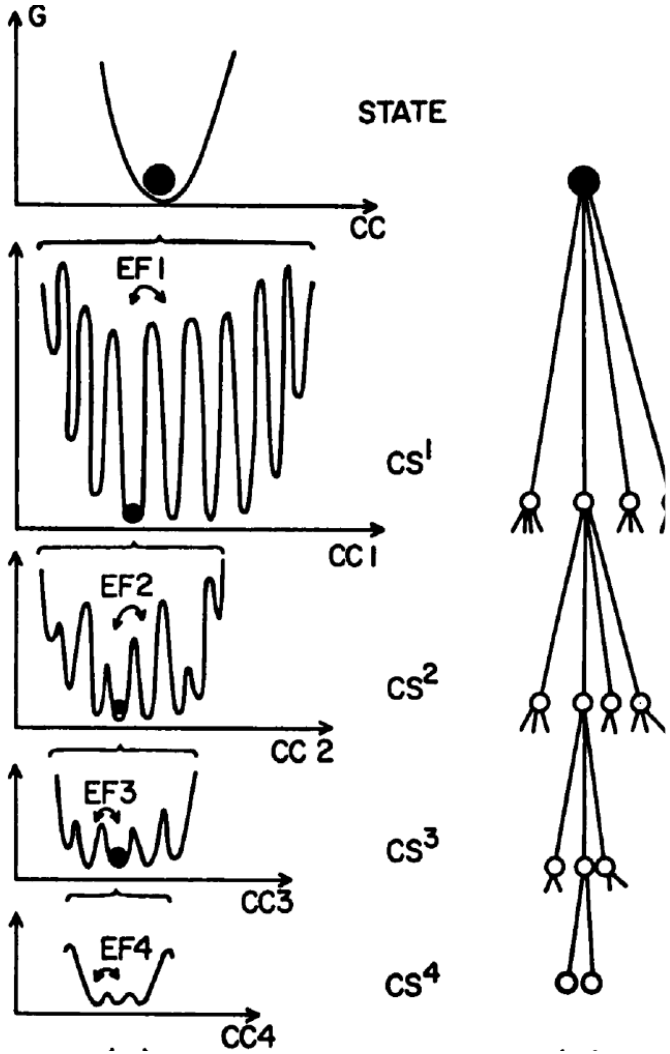

Myoglobin – the "hydrogene atom" of biophisics

- Myoglobin

Myoglobin (Mb) is an iron-containing protein found in the muscle tissue of mammals. Its physiological function relates to increased oxygen transport to muscle and oxygen storage. Mb was the first protein to have its three-dimensional structure revealed by the X-ray crystallography (John Kendrew, Nobel prize in chemistry 1962).

Myoglobin contains the porphyrin complex of Fe. The iron atom oxidation bound to O_2 is +2 (gives the color of fresh meat). The iron atom in the oxidation state +3 gives the brown color (well done meat). The grilled meat can also take on a reddish pink ring that comes from the heme center binding to carbon monoxide -CO. The ligand binding causes substantial structural change at the porphyrin complex center, which shrinks in radius and the Fe atom moves into the center of the N4 pocket. Such changes in spectrum allows directly detect the state of the reaction centrum.

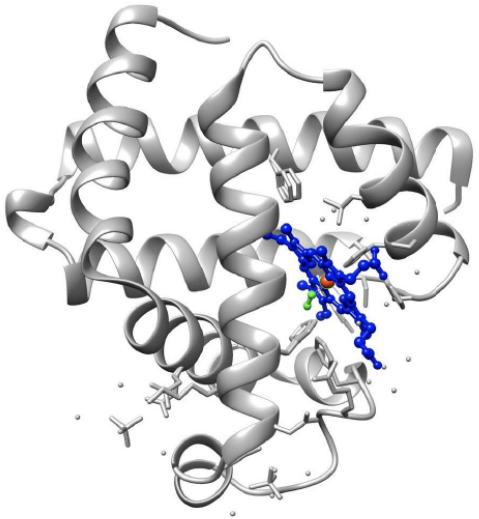

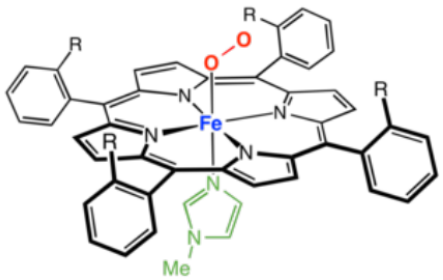

CO- rebinding kinetics to Mb

- MbCO (in 75% glycerol solvent) is photodissociated at a temperature T into highly excited unbounded state Mb*, which further relaxes to a bunch of functionally-active conformation states Mb1, where the CO-ligand rebinding becomes possible. The evolution of markers characterizing the unbounded protein concentration S(t) (survival probability) is followed as a function of temperature and time after photodissociation.

$$\mathrm{MbCO} \overset{h\nu}{\rightsquigarrow} [\mathrm{Mb}^* \to \ldots \to \mathrm{Mb}_1] \overset{\mathrm{CO}}{\to} \mathrm{MbCO}$$

- The kinetics has unexpected temperature dependance: It becomes faster with increasing the temperature up to 170 K. It slows down above 170 K and transforms from power-law to exponential decay.

P.J. Steinbach et. al., Biochemistry 30, 3988 (1991)

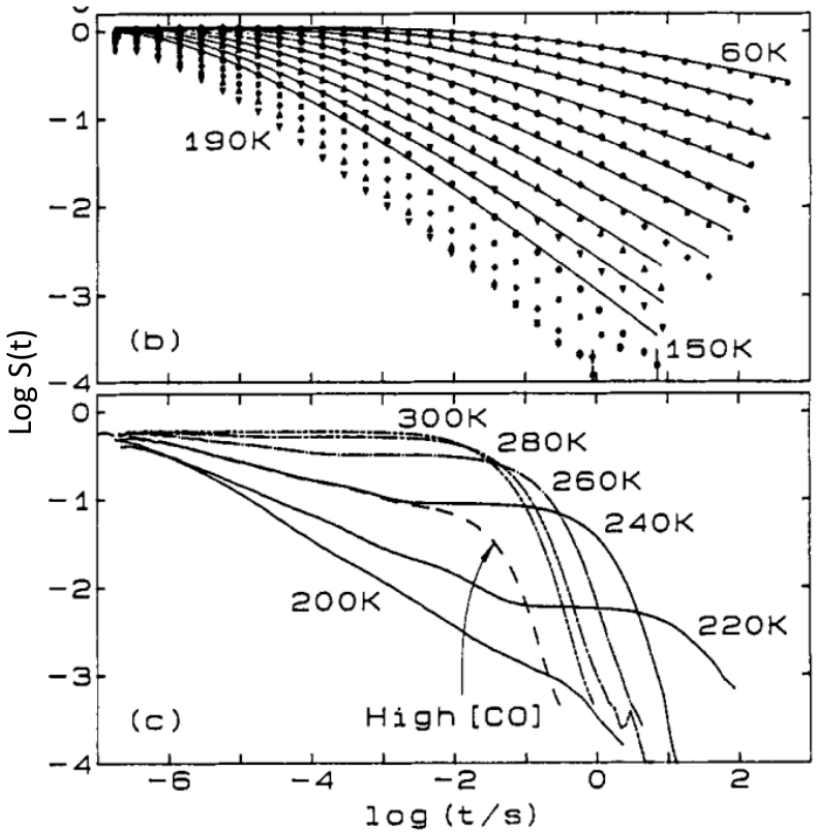

p-Adic model

- Conformational rearrangements are restricted to a bounded region of the conformational space of the system and this region is the *p*-adic disk

$$B_r = \{x : |x|_p \leqslant p^r, r > 1\}$$

- The hierarchical landscape is linear, i.e. conformational rearrangements are described by the Vladimirov operator
- In the region *Br*, there is a certain set of conformational states in which the system can undergo irreversible transformations. This set of states is described by the unit disc *Zp*. In other words, there is a reaction-type sink at each point of the disc *Zp*.
- The rate of the reaction sink at each point of the disc *Zp* is proportional to the mean value of the population density on that disc.
- The initial distribution *f (x, 0)* is constant on the *p*-adic layer

$$R_{\sigma\delta} = \left\{x : p^{\delta+1} \leqslant |x|_p \leqslant p^{\sigma},\ 0 \leqslant \delta < \sigma < r\right\}$$

$$f(x,0) = AG_{\delta}^{\sigma}(x) \equiv A\left[\Omega\left(|x|_p p^{-\sigma}\right) - \Omega\left(|x|_p p^{-\delta}\right)\right]$$

$$A^{-1} = p^{\sigma} - p^{\delta} \quad 0 \leqslant \delta < \sigma$$

- The observable (survival probability) is the integral $S(t) = \int_{Q_p} f(x,t)\,\mathrm{d}\mu(x)$

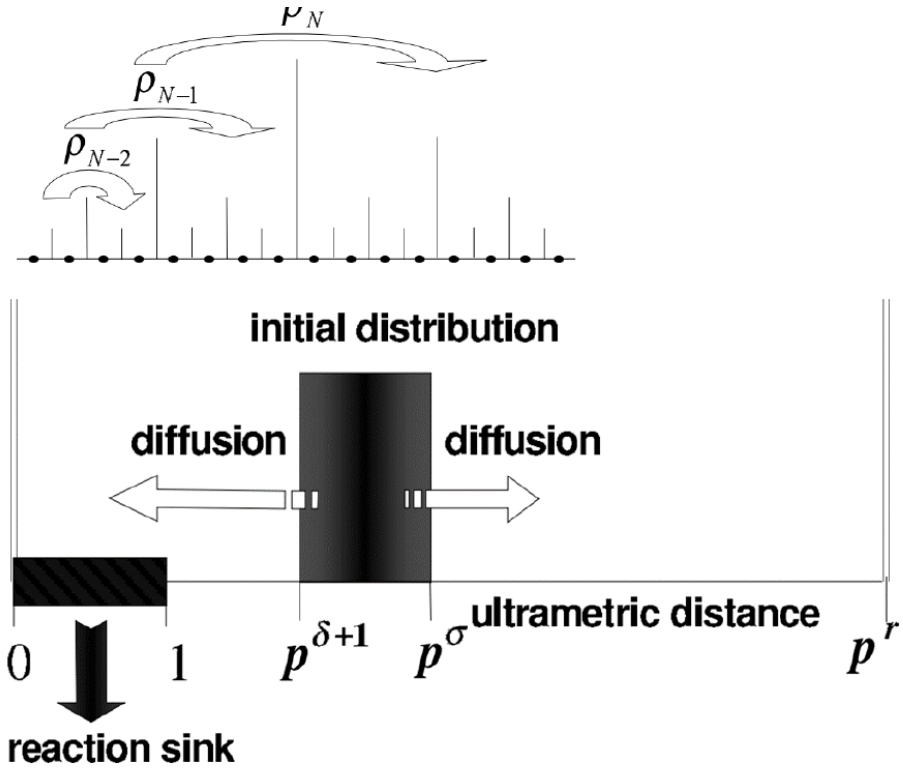

Theory and experiment comparizon

At high temperatures (curve 1) the distribution $f(x, t)$ reaches quasi-equilibrium very fast in the whole volume, i.e. during the observation period of time the function $f(x, t)$ is close to a homogeneous distribution and the population decays exponentially with the rate determined by the reaction rate.

As the temperature decreases (curves 2 and 3), a small section of power relaxation appears on the curve $S(t)$ and then extends to the major part of the time window. In this case, the kinetics $S(t)$ is limited first by the ultrametric diffusion (power section of S) and then by the reaction sink (exponential decay).

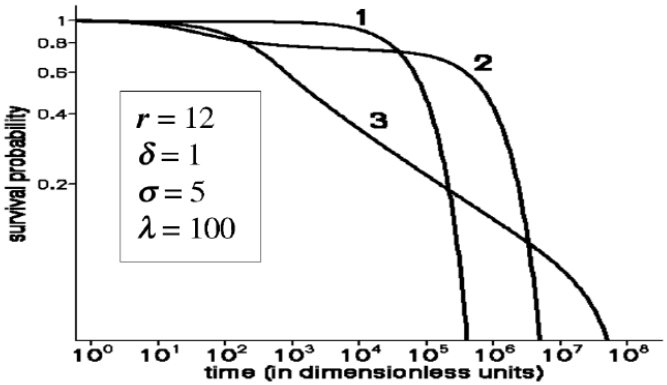

$\alpha = 0.1$ (1), $\alpha = 0.7$ (2) and $\alpha = 1.2$ (3)

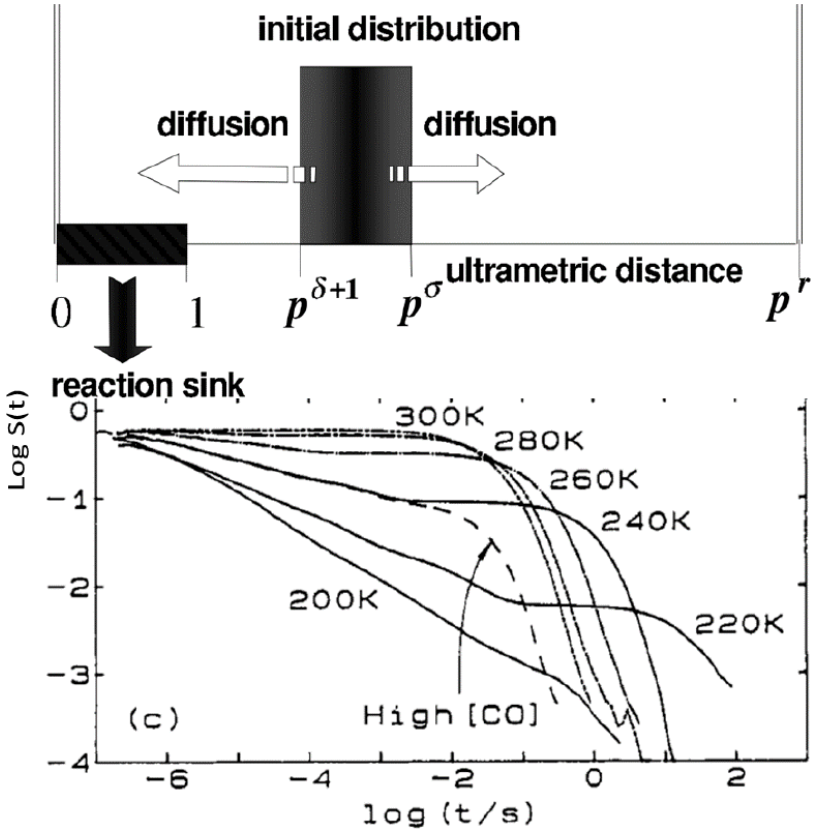

A Avetisov, A H Bikulov, S V Kozyrev and V A Osipov J. Phys. A: Math. Gen. 35 (2002) 177–189

p-adic diffusion equation:

$$\frac{\partial f(x,t)}{\partial t} = D_x^{\beta} f(x,t)$$

where $x \in \mathbb{Q}_p$, $t \in \mathbb{R}$, $\beta \sim \frac{1}{T}$. Offers an accurate and universal description of the **protein conformation dynamics**. The description takes into account the symmetry properties (hierarchical self-similarity) of the state space only.

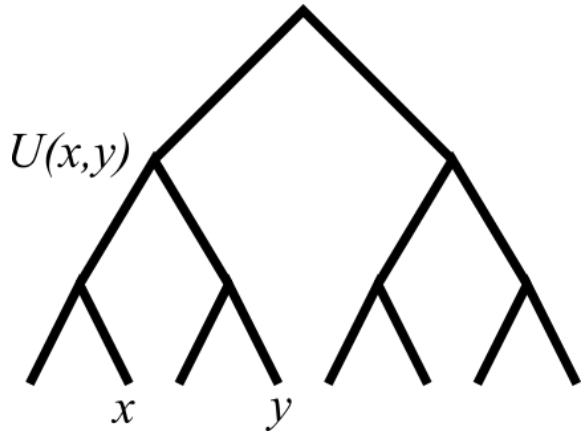

The ultrametric diffusion equation with a drift term:

$$\frac{\partial f(x,t)}{\partial t} = \int_X d\mu(y) \frac{e^{-\beta U(|x,y|)}}{|x,y|} \left(e^{\beta E(y)} f(y,t) - e^{\beta E(x)} f(x,t) \right)$$

It describes diffusion on an arbitrary hierarchical energy landscape. The additional terms generate a drift in the space.

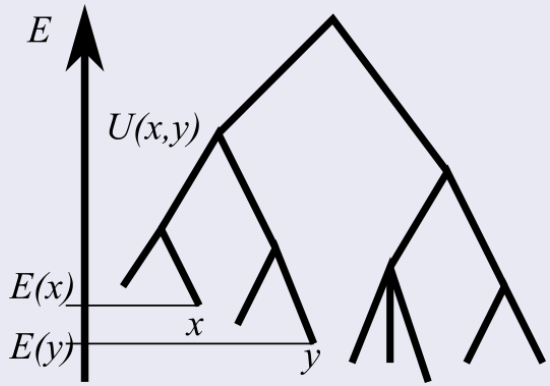

Block-rectangular hierarchical matrix

Block-rectangular hierarchical matrix:

$$\left(\begin{array}{cc|c|cc|c} \begin{array}{cc} q_0 & q_1 \\ q_0 & q_1 \end{array} & \begin{array}{cc} q_0 & q_1 \\ q_0 & q_1 \end{array} & & \begin{array}{cc} q_0 & q_1 \\ q_0 & q_1 \end{array} & \begin{array}{cc} q_0 & q_1 \\ q_0 & q_1 \end{array} & \\ \begin{array}{cc} q_1 & q_0 \\ q_1 & q_0 \end{array} & \begin{array}{cc} q_1 & q_0 \\ q_1 & q_0 \end{array} & q_2 & \begin{array}{cc} q_1 & q_0 \\ q_1 & q_0 \end{array} & \begin{array}{cc} q_1 & q_0 \\ q_1 & q_0 \end{array} & q_2 \\ \hline & & & & & \\ & \begin{array}{cc} q_0 & q_1 \\ q_0 & q_1 \end{array} & & & \begin{array}{cc} q_0 & q_1 \\ q_0 & q_1 \end{array} & \\ q_2 & \begin{array}{cc} q_1 & q_0 \\ q_1 & q_0 \end{array} & & q_2 & \begin{array}{cc} q_1 & q_0 \\ q_1 & q_0 \end{array} & \end{array}\right).$$

Here q_2 is a 4×2 matrix. The model describes ultrametric diffusion with a constant drift.

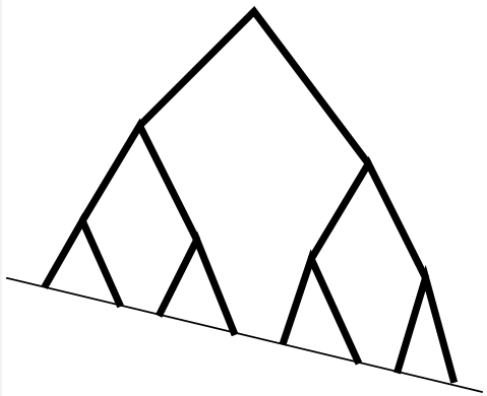

Parisi matrix as an operator on a set of symbolic sequences

Tensor product representation of Parisi matrix.

Hilbert 2^r dimensional space: $\mathcal{H}_{2^r} = h \otimes h \otimes \cdots \otimes h$, let $\boldsymbol{\omega} \in \mathcal{H}_{2^r}$.

$$\hat{\boldsymbol{Q}}\boldsymbol{\omega} = \sum_{\gamma=0}^{r} a_\gamma \hat{\boldsymbol{S}}_\gamma \boldsymbol{\omega}, \qquad \hat{\boldsymbol{S}}_\gamma \boldsymbol{\omega} = \underbrace{\omega_1 \otimes \cdots \otimes \omega_{r-\gamma}}_{r-\gamma} \otimes \underbrace{\hat{\boldsymbol{s}}\omega_{r-\gamma+1} \otimes \cdots \otimes \hat{\boldsymbol{s}}\omega_r}_{\gamma},$$

where a_γ's are arbitrary, and $\hat{\boldsymbol{s}}$ is a projection: $\hat{\boldsymbol{s}}|1>=1|1>$, $\hat{\boldsymbol{s}}|0>=0|0>$.

$\hat{\boldsymbol{Q}}$ is a Parisi matrix in the basis of $|0>$ and $|1>$ and has eigenvalues $\lambda^{(\mu)} = \sum_{\gamma=0}^{\mu} a_\gamma$ with $\mathbf{mult}(\lambda^{(\mu)}) = 2^{r-\mu-1}$.

Translation operator $\hat{\boldsymbol{T}}$ It makes one step shift

$$\hat{\boldsymbol{T}}\omega_1 \otimes \cdots \otimes \omega_{r-1} \otimes \omega_r = \omega_r \otimes \omega_1 \otimes \cdots \otimes \omega_{r-1}, \qquad \omega_j \in h.$$

$$\hat{\boldsymbol{T}} = \begin{pmatrix} |1> & & & & |0> & & & \\ & |1> & & & & |0> & & \\ & & \cdot & & & & \cdot & \\ & & & \cdot & & & & \cdot \\ & & & & \cdot & & & \\ & & & & & \cdot & & \\ & & & |1> & & & & |0> \end{pmatrix},$$

Block-rectangular hierarchical matrices

The family of operators is introduced as the products

$$\hat{\mathcal{Q}} = \hat{\boldsymbol{T}}\hat{\boldsymbol{Q}},$$

Thus the evolution generated by $\hat{\mathcal{Q}}$ is a composition of ultrametric diffusion $\hat{\boldsymbol{Q}}$ and deterministic process induced by $\hat{\boldsymbol{T}}$.

$$\left(\begin{array}{c|c|c|c}
\begin{array}{cc} q_0 & q_1 \\ q_0 & q_1 \\ \hline q_1 & q_0 \\ q_1 & q_0 \end{array} & q_2 & \begin{array}{cc} q_0 & q_1 \\ q_0 & q_1 \\ \hline q_1 & q_0 \\ q_1 & q_0 \end{array} & q_2 \\ \hline
q_2 & \begin{array}{cc} q_0 & q_1 \\ q_0 & q_1 \\ \hline q_1 & q_0 \\ q_1 & q_0 \end{array} & q_2 & \begin{array}{cc} q_0 & q_1 \\ q_0 & q_1 \\ \hline q_1 & q_0 \\ q_1 & q_0 \end{array}
\end{array}\right).$$

Spectral problem.

The spectral problem for the matrix $\hat{\mathcal{Q}}$ for prime r

$$\Lambda^{(m;\boldsymbol{\nu};j)} = \begin{cases} \lambda^{(r)}, & m = r; \\ e^{2\pi \mathrm{i} j/r} \left(\lambda^{(0)}\right)^{1-m/r} \prod_{i=1}^{\ell} \left(\lambda^{(i)}\lambda^{(i-1)} \dots \lambda^{(1)}\right)^{\nu_i/r}, & 1 < m < r-1; \\ \lambda^{(0)}, & m = 0. \end{cases}$$

The corresponding multiplicities are given by

$$\mathbf{mult}\left(\Lambda^{(m;\boldsymbol{\nu})}\right) = \begin{cases} 1, & m = r; \\ \frac{(r-m-1)!}{(r-m-\sum_i \nu_i)! \prod_i \nu_i!}, & 1 < m < r-1; \\ (p-1)\left(1 + \frac{(p-1)^{r-1}-1}{r}\right) & m = 0. \end{cases}$$

where $\lambda^{(\mu)} = \sum_{\gamma=0}^{\mu} a_\gamma$ are eigenvalues of the Parisi matrix and ν_i is the constrained partition of m: $\sum_{i=1}^{\ell} i\nu_i = m$, such that $\sum_{i=1}^{\ell} \nu_i \leq r - m$.

Mapping onto the information disk model

The family of operators

$$\hat{\mathcal{Q}} = \hat{\boldsymbol{T}}\hat{\boldsymbol{Q}},$$

Thus the evolution generated by $\hat{\mathcal{Q}}$ is a composition of ultrametric diffusion $\hat{\boldsymbol{Q}}$ and deterministic process induced by $\hat{\boldsymbol{T}}$.

Ultrametric diffusion with a constant drift

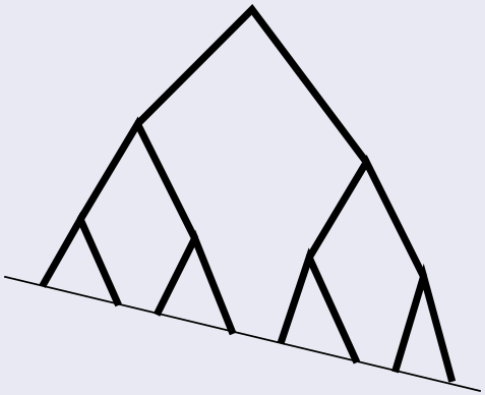

Initial stage of the process.

Errors generation model in information sequences

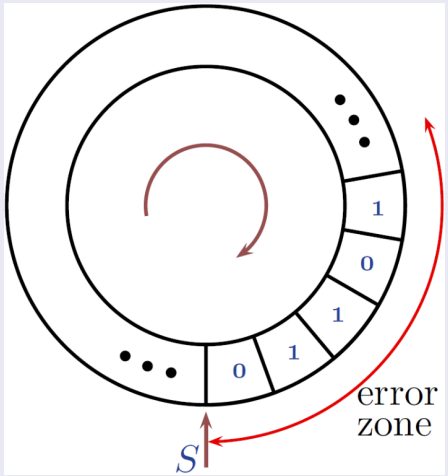

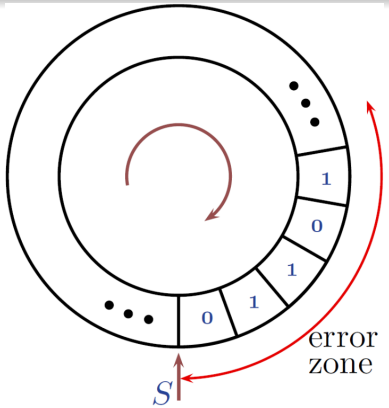

- The information carrier ("disk") consists of r cells. Each of them contains a digit $\{0,1\}$. At the discreet moments of time $t = 0, 1, \ldots$ disc rotates one step clockwise, at $t = \ell \leq r$ the pointer S points to the ℓth cell.
- The noise affects the cells placed "rightwards" to the point S. The probability to affect γ consecutive cells is given by a_γ ($\sum_{\gamma=0}^{r} a_\gamma = 1$). The content of each affected cell is replaced by any symbol from $\{0,1\}$ with equal probability.
- Each state of the disc can be described by a vector $\boldsymbol{w} \in \mathcal{H}_{2^r}$:

$$\boldsymbol{w}(t) = \sum_J w_J(t)|\boldsymbol{e}_J>, \qquad |\boldsymbol{e}_j>=\bigotimes_{k=1}^{r}|j_k\rangle, \qquad j_k \in \{0,1\},$$

  where $w_J(t)$ are probabilities to find the disc having informational content encoded by the sequence of symbols $J = [j_1 j_2 \ldots j_r]$.
- The result of ℓ steps time evolution is described by the operator

$$\prod_{i=1}^{\ell}\left[\hat{\boldsymbol{T}}\sum_{\gamma=0}^{r} a_\gamma \hat{\boldsymbol{S}}_\gamma\right] = (\hat{\boldsymbol{T}}\hat{\boldsymbol{Q}})^\ell = \hat{\mathcal{Q}}^\ell$$

Estimation of losses.

The moment generation function

An auxiliary operator $\hat{\boldsymbol{E}}$

$$\hat{\boldsymbol{E}} = (\mathbb{1} + e^{\alpha}\,\mathbb{P}) \otimes (\mathbb{1} + e^{\alpha}\,\mathbb{P}) \otimes \cdots \otimes (\mathbb{1} + e^{\alpha}\,\mathbb{P});$$
$$\mathbb{1} = |0\rangle\langle 0| + |1\rangle\langle 1|, \qquad \mathbb{P} = |0\rangle\langle 1| + |1\rangle\langle 0|,$$

so that $< J|\hat{\boldsymbol{E}}|J' >= e^{k\alpha}$, with k being the number of different symbols (compared pairwise) in the sequences J and J'.
The moment generation function

$$R_{\ell}(\alpha) =< J_0|\,\hat{\boldsymbol{T}}^{-\ell}\,\hat{\boldsymbol{E}}\,\hat{\mathcal{Q}}^{\ell}|J_0 > .$$

The mean value of the changes accumulated in the disk after ℓ rotations and its square displacement are

$$\begin{aligned} < k >_{t=\ell} &= \partial_{\alpha} R_{\ell}(\alpha)|_{\alpha=0}; \\ < (k - < k >)^2 >_{t=\ell} &= \partial_{\alpha}^2 R_{\ell}(\alpha)|_{\alpha=0} - < k >_{t=\ell}^2 . \end{aligned}$$

Number of errors statistics after full turn in case of Boltzmann noise.

The probabilities a_γ are proportional to $e^{-\beta\gamma}$ with parameter $\beta \sim 1/T$ (inverse temperature).

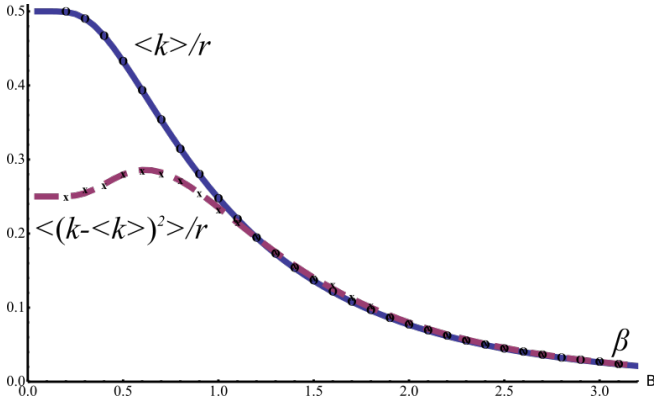

- $\beta \ll 1$: At high temperatures $< k > \sim \frac{r}{2}$ and $var(k) \sim \frac{r}{4}$. Almost every cell are affected. The probability that exactly k cells change their content is $2^{-r}\binom{r}{k}$ (Binomial distribution).
- $\beta \gg 1$: The randomising events caused by the noise are rare and mostly affect one cell only. One observes the equality $< k > \simeq var(k)$ (Poison process).
- $\beta \sim 1$: The variance reaches its maximal value.

Gutkin B., Osipov V.Al. J. Stat. Phys. 143 (2011) 72

Quantum chaos

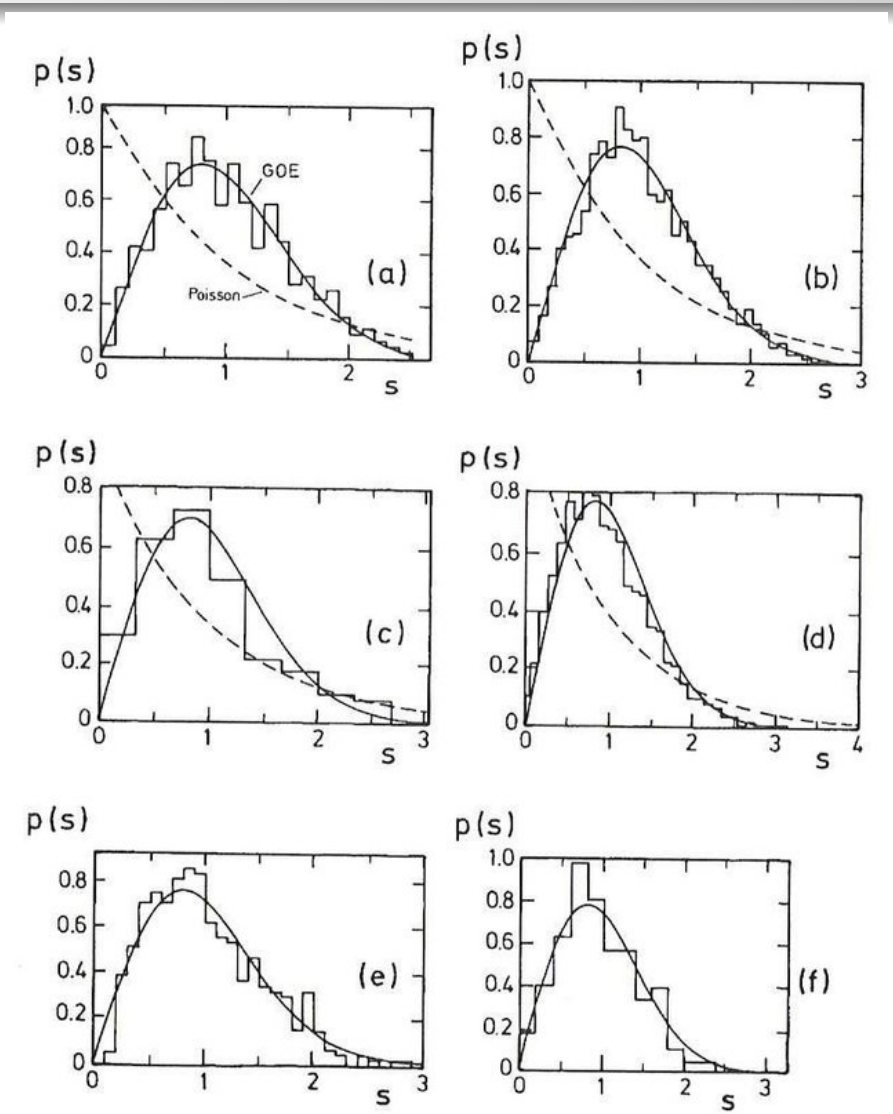

Eigenvalue spasing distributions for various quantum chaos systems.

Sinai Billiard (a), a hydrogen atom in a strong magnetic field (b), a NO_2 molecule (c), acoustic modes of a Sinai shaped quartz block (d), a chaotic microwave cavity (e), vibration modes of a stadium shaped plate (f). Both classical and quantum systems can be modelled with the Wigner distribution,

$$p(s) = s^{\beta} e^{-\xi s^2}$$

Periodic orbits in Quantum chaos

- One interested in statistics (correlations) of energy levels of a chaotic quantum system.
- Gutzwiller trace formula ($\hbar \to 0$), the density of energy levels

$$\rho(E) = \sum_n \delta(E - \varepsilon_n) \simeq \underbrace{W(E)}_{\text{smooth part}} + \mathrm{Re} \sum_{\gamma \in P.O.} \mathcal{A}_\gamma \exp\left(\frac{i}{\hbar} S_\gamma(E)\right)$$

S_γ is the classical action calculated along the periodic orbit γ, $\mathcal{A}_\gamma$ includes inverse density of neighbouring trajectories.

- Form factor **correlations of** ε_n $\Leftrightarrow$ **correlations of** S_γ

$$\mathcal{K}(\tau) = \int d\varepsilon e^{-i\varepsilon\tau} < \rho(E+\varepsilon)\rho(E-\varepsilon) > \simeq \sum_{\gamma\gamma'} \mathcal{A}_\gamma \mathcal{A}^*_{\gamma'} \exp\left(\frac{i}{\hbar} \Delta S_{\gamma\gamma'}(E,\varepsilon)\right)$$

- Classification of trajectories with respect to their contribution?

$$\mathcal{K}(\tau) = \int d\varepsilon e^{-i\varepsilon\tau} < \rho(E+\varepsilon)\rho(E-\varepsilon) > \simeq \sum_{\gamma\gamma'} \mathcal{A}_\gamma \mathcal{A}^*_{\gamma'} \exp\left(\frac{i}{\hbar}\Delta S_{\gamma\gamma'}\right)$$

Classification of trajectories on their contribution:

1. diagonal approximation by Berry, $\gamma = \gamma'$;
2. Sieber-Richter pairs, $\gamma \neq \gamma'$ $\exists$ encounter;

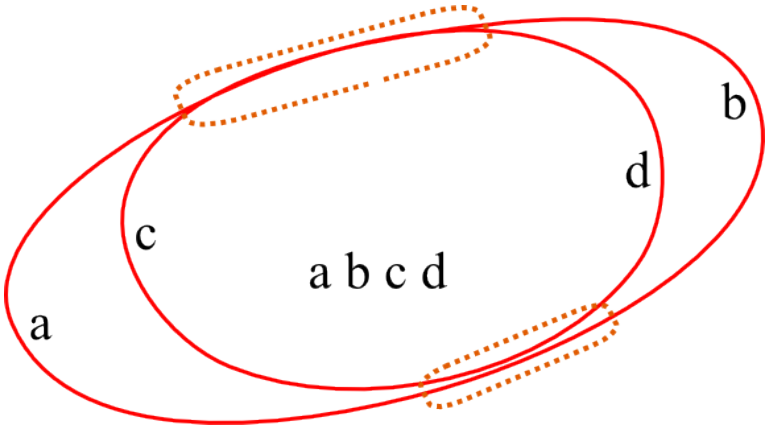

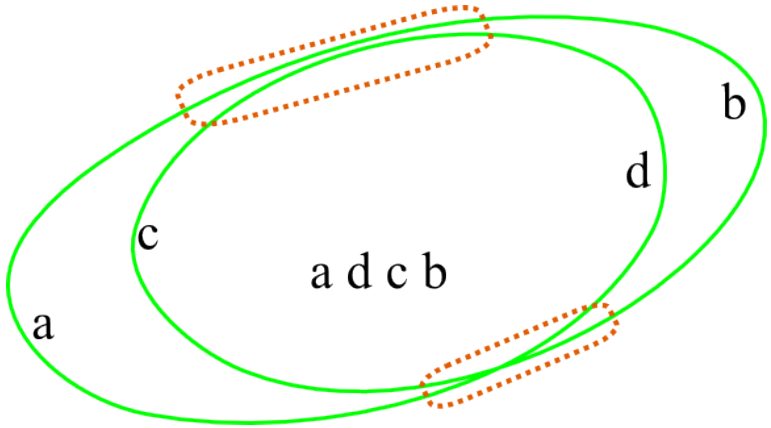

Backer's map

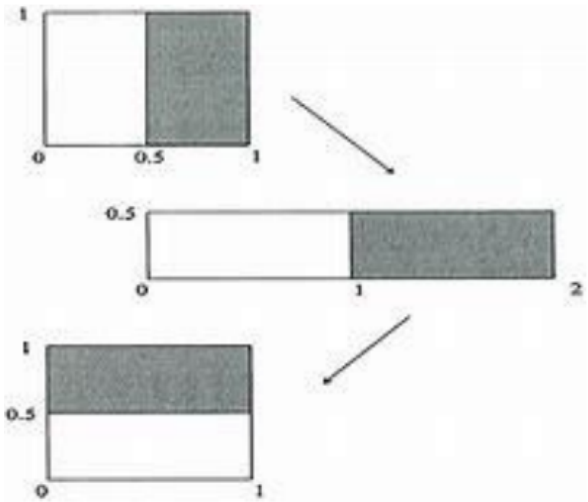

$$(x_{n+1}, y_{n+1}) = \begin{cases} \left(2x_n, \frac{y_n}{2}\right), & 0 \le x_n < \frac{1}{2}; \\ \left(2 - 2x_n, 1 - \frac{y_n}{2}\right), & \frac{1}{2} \le x_n \le 1. \end{cases}$$

- Trajectory is encoded by a bi-infinite binary sequence 01100011.11101001
- The evolution is generated by the left-shift operator;
- The rational sequence corresponds to the periodic orbit.

The frequency representation of sequences.

We do not interested in absolute position of symbols in the sequence. The local filling is of our interest.

The simplest chaotic system is the Backer's map: any cyclic symbolic sequence encodes the periodic orbit.
Example: the cyclic sequence [001],

$$\begin{pmatrix} 0 \\ 0 \\ 1 \end{pmatrix} \qquad \begin{array}{ll} [00] & 1 \\ [01] & 1 \\ [10] & 1 \\ [11] & 0 \end{array}$$

The vector of frequencies $x_{2\,(3)} = (1\ 1\ 1\ 0)$ contains information about the encounters.

p-close sequences

p-closeness ($\gamma \overset{p}{\sim} \beta$)

Two cyclic sequences of equal lengths, γ and β, are p-close if their frequency vectors are equal $x_p[\gamma] = x_p[\beta]$.

Properties of $\overset{p}{\sim}$

- If $\gamma \overset{p}{\sim} \alpha$ and $\gamma \overset{p}{\sim} \beta$, then $\alpha \overset{p}{\sim} \beta$ (transitivity);
- If $\gamma \overset{p+1}{\sim} \alpha$ then $\gamma \overset{p}{\sim} \alpha$ (nesting).

All symbolic sequences of a given length can be distributed over hierarchically nested clusters.

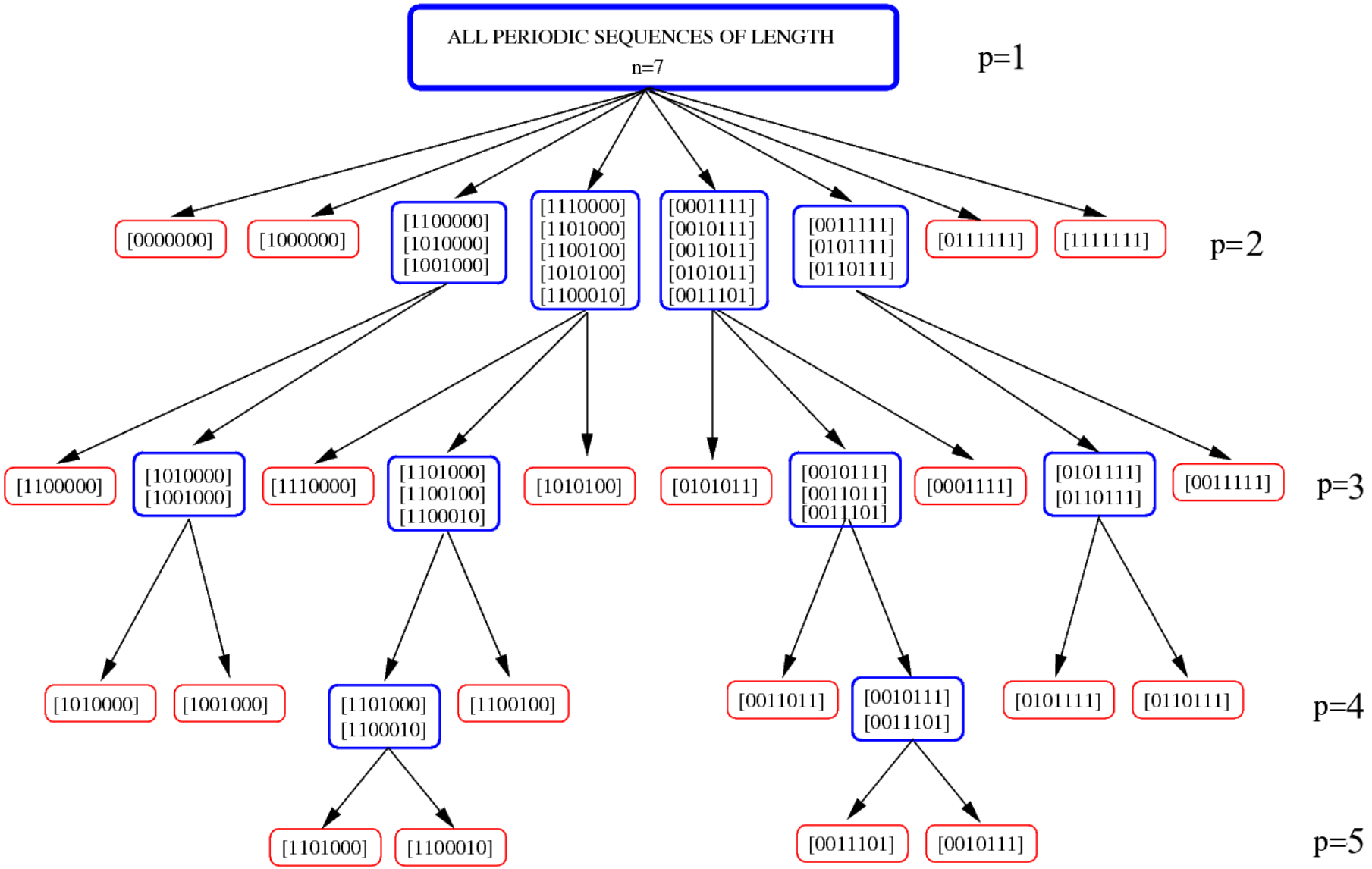
ALL PERIODIC SEQUENCES OF LENGTH
n=7
p=1
[0000000]
[1000000]
[1100000]
[1010000]
[1001000]
[1110000]
[1101000]
[1100100]
[1010100]
[1100010]
[0001111]
[0010111]
[0011011]
[0101011]
[0011101]
[0011111]
[0101111]
[0110111]
[0111111]
[1111111]
p=2
[1100000]
[1010000]
[1001000]
[1110000]
[1101000]
[1100100]
[1100010]
[1010100]
[0101011]
[0010111]
[0011011]
[0011101]
[0001111]
[0101111]
[0110111]
[0011111]
p=3
[1010000]
[1001000]
[1101000]
[1100010]
[1100100]
[0011011]
[0010111]
[0011101]
[0101111]
[0110111]
p=4
[1101000]
[1100010]
[0011101]
[0010111]
p=5

Periodic sequences of the length $n = 11$

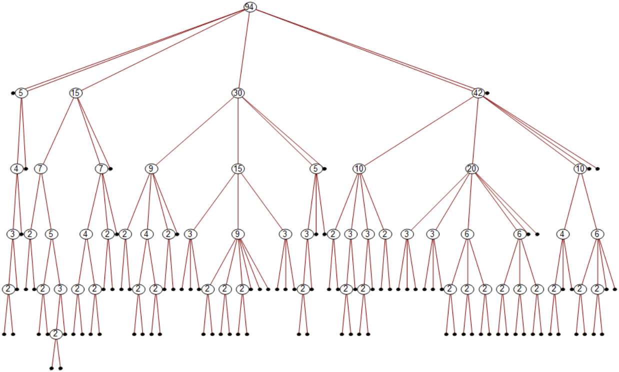

Clustering of cyclic binary sequences of the length $n = 11$ (only half of the tree, 94 sequences out of 188, is shown). The end-points represent the sequences, the numbers in the circles give the total number of sequences in the corresponding cluster.

The maximal branching level of the tree is $p_{max} = \lceil \frac{n-3}{2} \rceil + 1$.

Ultrametrics on a set of cyclic symbolic sequences

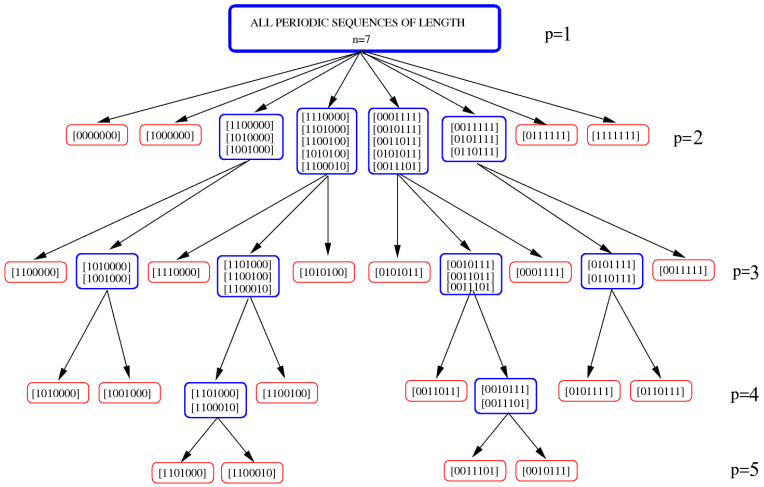

Ultrametric distance on the set of cyclic symbolic sequences:

$$d(\alpha,\beta) = e^{-p_{\max}} \qquad p_{\max} = \max_{\alpha \overset{p}{\sim} \beta}(p)$$

$$d(\alpha,\beta) \le d(\alpha,\gamma) + d(\beta,\gamma);$$

$$d(\alpha,\beta) \le \max\Big(d(\alpha,\gamma), d(\beta,\gamma)\Big).$$

What are statistics of clusters?

Some results regarding the cluster sizes

- The total number of clusters in the regime of finite p and $n \gg 1$ grows as $\frac{1}{4} n^{2^{p-1}} (1 + O(1/n))$
- The asymptotic for the average sizes of clusters, $< \|\mathcal{C}\| >$.
  – For $n \lesssim \sqrt{2^p}$ the average cluster size is one, $< \|\mathcal{C}\| > \approx 1$, and the number of clusters is almost equal to the total number of cyclic sequences.
  – For $2^{p/2} \ll n \ll 2^p$ one can find that $\log < \|\mathcal{C}\| > \sim n^2$.
  – For $n \gg 2^p$ the average size is $< \|\mathcal{C}\| > = \frac{2^n}{n} \left(\frac{2^{p-1}}{n\pi} \right)^{2^{p-2}} (1 + O(1/n))$.
  Further growth of n gives $\log < \|\mathcal{C}\| > \sim n$.

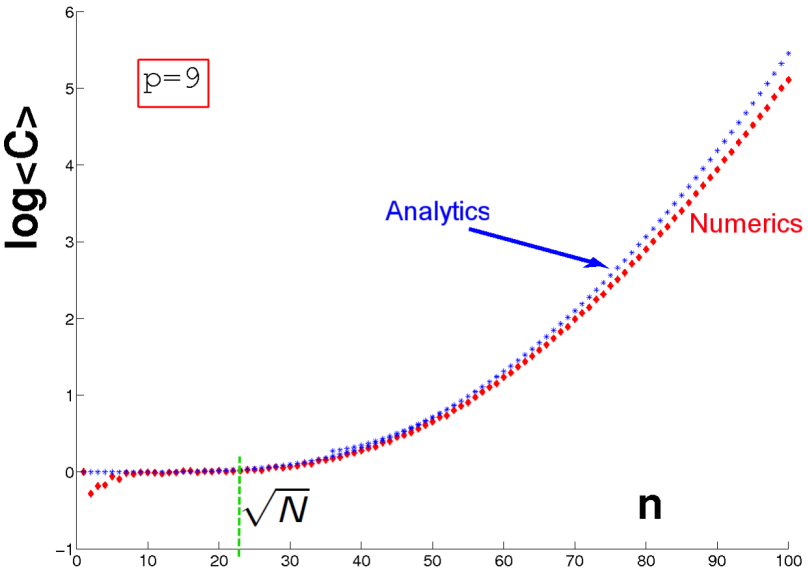

$(N = 2^{p-1} = 256)$

Some results regarding the cluster distributions

- The size of the largest cluster, $\|\mathcal{C}_{\max}\|$ in the limit of long sequences $n \gg 1$ and finite p behaves like $\|\mathcal{C}_{\max}\| = \left(\frac{2^n}{n}\right)\left(\frac{2^p}{\pi n}\right)^{2^{p-2}}\left(1+O(n^{-1})\right)$.
- The probability density that a randomly chosen cyclic sequence belongs to a cluster of the size less then $t\,\|\mathcal{C}_{\max}\|$, $t \in [0,1]$, it is $(n \gg 1)$

$$\rho(t) = \frac{(-\log t)^{2^{p-2}-1}}{(2^{p-2}-1)!}.$$

- Probability to find k randomly chosen sequences of the same length to be belonging to the same cluster: $\left(\frac{1}{k}\right)^{2^{p-2}}\left(\frac{2^p}{\pi n}\right)^{(k-1)2^{p-2}}\left(1+O(n^{-1})\right)$.

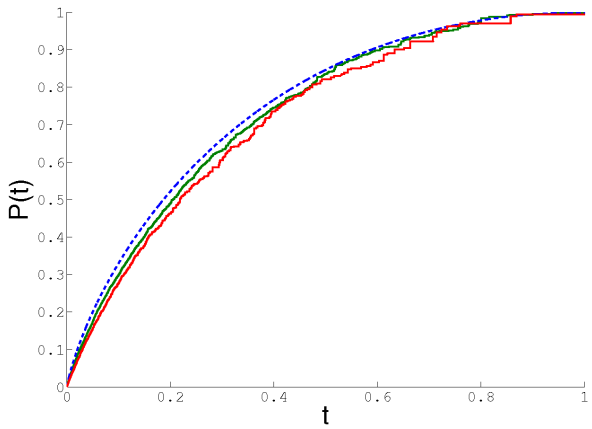

Gutkin B., Osipov V.Al. Nonlinearity 26 (2013) 177

Exact distribution of cluster sizes for the case $p = 3$ at $n = 70$ (upper green) and $n = 47$ (lower red) is shown in comparison with the asymptotic expression $P(t) = t(1 - \log t)$ (dashed blue line) and $t\,\|\mathcal{C}_{\max}\|$, $t \in [0,1]$,.

Exactly solvable many-body quantum chaos model

- We consider D-dimensional (below D=2) lattice of interacting quantum particles with individual chaotic behavior, which evolves in discrete time-steps. The Hamiltonian

$$H(t) = H_I + H_K \sum_{\tau=-\infty}^{+\infty} \delta(t-\tau)$$

- H_I – interaction of the nearest neighbor particles.
- H_K – the kick part induces independent chaotic evolution of non-interacting particles in L-dimensional Hilbert space. The total basis

$$\left\{ |\boldsymbol{s}\rangle \equiv \prod_{n=1}^{N} \prod_{m=1}^{M} |s_{n,m}\rangle\,, \quad s_{n,m} = \overline{1,L} \right\}$$

$N \times M$ lattice

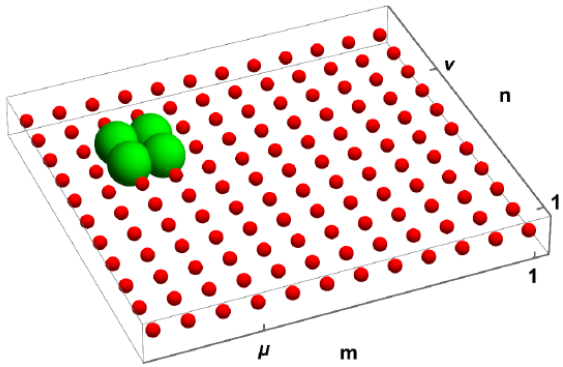

- The Floquet evolution operator acts in the discrete time-steps, at each step the evolution is a product of two unitary operators:

$$U = U_K U_I$$

- The main object of our consideration is the correlation function

$$C(\boldsymbol{r},t) = \langle \hat{Q}_1(0)\hat{Q}_2(t)\rangle - \langle \hat{Q}_1(0)\rangle \langle \hat{Q}_2(t)\rangle$$

$$\langle\cdot\rangle = \frac{1}{L^2}\mathrm{Tr}\,(\cdot)$$
$$\hat{Q}(t) = U^{-t}\hat{Q}U^t$$

Exactly solvable many-body quantum chaos model

- The Hamiltonian $$H(t) = H_I + H_K \sum_{\tau=-\infty} \delta(t-\tau)$$

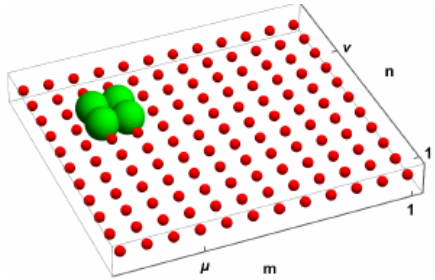

- The total basis $$\left\{ |s\rangle \equiv \prod_{n=1}^{N} \prod_{m=1}^{M} |s_{n,m}\rangle\,, \quad s_{n,m} = \overline{1,L} \right\}$$
- The Floquet evolution operator acts in the discrete time-steps, at each step the evolution is a product of two unitary operators: $U = U_K U_I$
- The Kick operator mixes the quantum states of a single particle

$$\langle \boldsymbol{s}|U_K|\boldsymbol{s}'\rangle = \prod_{n=1}^{N} \prod_{m=1}^{M} \langle s_{n,m}|u[g]|s'_{n,m}\rangle$$

Unitary matrix with a symbol g

$$\langle s|u[g]|s'\rangle = \frac{1}{\sqrt{L}} e^{ig(s,s')}$$

$$\frac{1}{L}\sum_{s'=1}^{L} e^{ig(s,s')} e^{-ig^*(s'',s')} = \delta(s,s'')$$

- The Interaction operator is diagonal, it only adds a phase to the evolution

$$\langle \boldsymbol{s}|U_I|\boldsymbol{s}'\rangle = \delta(\boldsymbol{s},\boldsymbol{s}') \exp\left\{ \mathrm{i} \sum_{n=1}^{N} \sum_{m=1}^{M} \left[f_h(s_{n,m}, s_{n+1,m}) + f_v(s_{n,m}, s_{n,m+1}) \right] \right\}$$

Exactly solvable many-body quantum chaos model

The unitary evolution operator acts in the discrete time-steps, the single step evolution is a product $U = U_K U_I$

$$\langle \boldsymbol{s}|U_I|\boldsymbol{s}'\rangle = \delta(\boldsymbol{s},\boldsymbol{s}')\exp\left\{\mathrm{i}\sum_{n=1}^{N}\sum_{m=1}^{M}\left[f_h(s_{n,m},s_{n+1,m})+f_v(s_{n,m},s_{n,m+1})\right]\right\}$$

$$\langle \boldsymbol{s}|U_K|\boldsymbol{s}'\rangle = \prod_{n=1}^{N}\prod_{m=1}^{M}\langle s_{n,m}|u[g]|s'_{n,m}\rangle$$

Dual evolution operators

$$U = U_K[g]U_I[f_h,f_v]$$

$$\tilde{U} = U_K[f_v]U_I[f_h,g] \qquad \tilde{U} = U_K[f_h]U_I[g,f_v]$$

The operators with tilde are not necessary unitary.

The operators with tilde are unitary if the matrices with the symbols g, f_h and f_v are unitary and satisfy the Hadamard property: $u^\dagger = u$, and $\left|u_{i,j}\right| = \left|u_{k,\ell}\right|$.

Exactly solvable many-body quantum chaos model

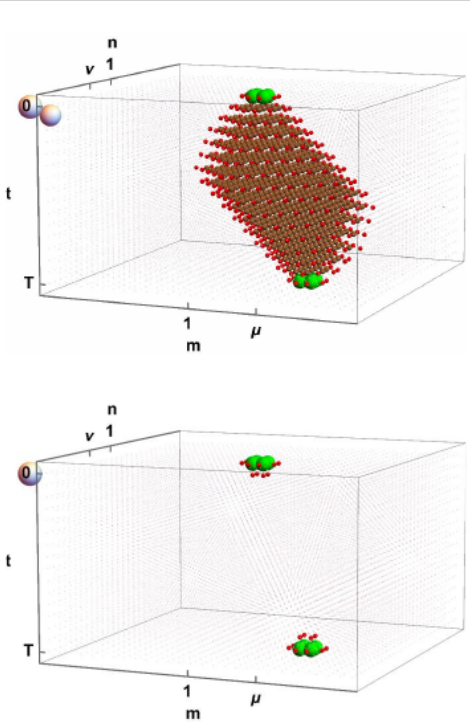

In the completely dual unitary case the correlation function nullifies inside and outside of the space-time cone. $|t| \geq |n| + |m|$

$$|m| \geq |n| + |t| \quad |n| \geq |t| + |m|$$

The only solution is $t = m = n = 0$
For the partially dual case only two inequalities

$$|t| \geq |n| + |m| \quad \cap \quad |n| \geq |t| + |m|$$

The only possible location of the non-trivial correlations is the cone edge.

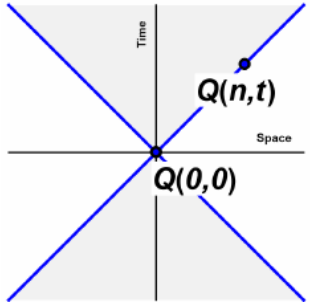

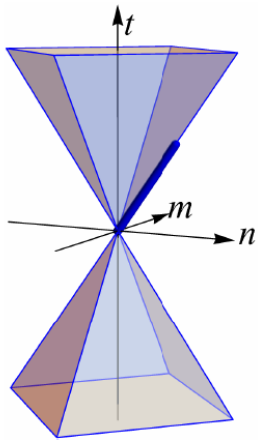

The problem of correlation function for the partially unitary dual quantum chaotic map is exactly solvable.

$$C(t) = < \mathbf{\Phi}_{init} | \hat{T}^{t-2} | \mathbf{\Phi}_{final} > \propto \lambda_1^t \propto e^{-t|\ln \lambda_1|}$$

The operators with tilde are not necessary unitary.

The kicked Ising spin-lattice model

The interaction and kicked Hamiltonians in the minimal dimension Hilbert space (L=2) for the partially unitary-dual Ising model with an external magnetic field

$$H(t) = H_I + H_K \sum_{\tau=-\infty}^{+\infty} \delta(t-\tau) \qquad H_K = \frac{\pi}{2} \sum_{n=1}^{N} \sum_{m=1}^{M} \hat{\sigma}^x_{n,m}$$

$$H_I = \frac{\pi}{4} \sum_{n=1}^{N} \sum_{m=1}^{M} \hat{\sigma}^z_{n,m} \hat{\sigma}^z_{n+1,m} + \sum_{n=1}^{N} \sum_{m=1}^{M} \left[d_h \hat{\sigma}^z_{n,m} \hat{\sigma}^z_{n,m+1} + h \hat{\sigma}^z_{n,m} \right]$$

Initial and final states are connected by a line composed of identical unit cells along the light-cone adge

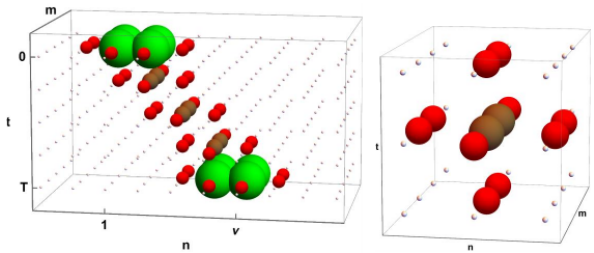

Pauli matrices

$$\hat{\sigma}^z = \begin{pmatrix} 1 & 0 \\ 0 & -1 \end{pmatrix}, \quad \hat{\sigma}^x = \begin{pmatrix} 0 & 1 \\ 1 & 0 \end{pmatrix}, \quad \hat{\sigma}^y = \begin{pmatrix} 0 & -\mathrm{i} \\ \mathrm{i} & 0 \end{pmatrix}$$

Spatiotemporal duality

$$u[g] = \frac{1}{\sqrt{2}} \begin{pmatrix} 1 & -\mathrm{i} \\ -\mathrm{i} & 1 \end{pmatrix}$$

$$u[f_v] = e^{\mathrm{i}\pi/4} u[g]$$

$$u[f_h] = \frac{1}{\sqrt{2}} \begin{pmatrix} e^{-\mathrm{i}(d_h+h)} & e^{\mathrm{i}d_h} \\ e^{\mathrm{i}d_h} & e^{-\mathrm{i}(d_h-h)} \end{pmatrix}$$

Hadamard unitary matrix

$$u^\dagger = u \quad \forall i,j,k,\ell: \ |u_{i,j}|^2 = |u_{k,\ell}|^2$$

The transfer matrix has block hierarchical structure

$$C(t) = < \Phi_{init} | \hat{T}^{t-2} | \Phi_{final} >$$

$T =$